

HIGH ACCURACY IMAGE ROTATION AND SCALE ESTIMATION USING RADON TRANSFORM AND SUB-PIXEL SHIFT ESTIMATION

Takanori Fujisawa, Masaaki Ikehara

EEE Dept., Keio Univ., Yokohama, Kanagawa 223-8522, Japan

Email: {fujisawa, ikehara}@tkhm.elec.keio.ac.jp

ABSTRACT

Rotation and scale estimation of images are fundamental tasks in image registration. The conventional estimation method uses log-polar transform and 1D shift estimation to estimate rotation and scale regardless of the shift of images. However, this transform requires interpolation of the frequency components, which causes estimation error. We propose a rotation and scale estimation algorithm based on Radon transform and sub-pixel shift estimation. Radon transform can estimate the rotation independent of the shift and can reduce the influence of interpolation error because it is performed on the spatial image rather than the frequency. In addition, sub-pixel shift estimation using linear approximation of the phase component improves the precision of 1D shift estimation and achieves accurate rotation estimation. The proposed method was evaluated on test images, and the results demonstrate that the proposed method accurately estimates rotation compared to log-polar-based and other conventional methods.

Index Terms — Image registration, Rotation estimation, Scale estimation, Phase only correlation

1. INTRODUCTION

With the recent advancements in hardware technology, processing huge volumes of image and video data has become common. Image registration, which matches two or more images, is an important technology. These images are taken from, for example, video frames, different cameras, or different viewpoints, and image registration can be used in many applications, such as medical image analysis, object recognition, and industrial vision.

The fundamental task in image registration is to estimate the shift, scale, and rotation between two images. Conventional approaches for rotation and shift estimation are categorized by phase-only correlation (POC) approaches [1–5], intensity-based registration [6, 7], and feature-based registration [8]. The intensity-based image registration proposed by Thevenaz et al [9, 10]. A typical intensity-based algorithm maximizes Mattes' mutual information [6] using step gradient descent or a one-plus-one evolutionary algorithm [7].

The feature-based approach extracts the speeded-Up robust features (SURF) [11] or binary robust invariant scalable keypoints (BRISK) [12] and estimates a transform matrix using existing methods [8, 13, 14]. The intensity-based approach compares two images by plain and achieves high precision if the rotation angle is small and the scale is close to 1. However, to estimate a large angle or scale, the number of iterations required to calculate the optimization problem increases, and an incorrect estimation may be obtained because of a local solution. The feature-based approach depends on the number of features extracted from the images and the precision of the point-to-point estimation of features. Therefore, the

precision of the feature-based approach is reduced when a small number of feature points are extracted or incorrect matching occurs in point-by-point estimation. POC is a common method for image shift estimation [1, 2] that calculates the cross-power spectrum of the frequency of two images. The image shift is represented as the peak of this spectrum, and shift estimation is achieved by searching this peak. To estimate the rotation, a method that combines a log-polar transform and 1D POC has been proposed [3, 15, 16]. These methods translate the frequency of the image into a polar coordinate. The image rotation is represented as a horizontal dimensional shift in this coordinate. Note that the amount of shift does not depend on the scaling or spatial shift of the image. On this basis, the rotation estimation is achieved by estimating the horizontal shift by the 1D POC. However, log-polar transform must approximate the frequency components using an interpolation algorithm, and the approximation precision deteriorates significantly in high-frequency components, which results in low precision for the estimated rotation.

We improve the accuracy of the rotation estimation by introducing a new algorithm based on spatial Radon transform and sub-pixel estimation in the phase domain. In the proposed method, input images are transformed by Radon transform. As well as log-polar transform, the rotation of the image is represented as a horizontal shift. On this bases, we estimate the degree of rotation by estimating the shift on the transformed images. Radon transform can be calculated in the spatial domain, and interpolation of the frequency component is not required. In addition, Radon transform sums all pixels along the specified angle, which reduces the error caused by interpolating the image pixels. Furthermore, we introduce a high-accuracy shift estimation based on the linear approximation of the phase component. Conventional algorithms search the peak of the POC by fitting a model function. In the estimation of discrete images, the precision of this search is limited to the integer. The proposed approach estimates the shift by linear approximation of the phase component. This method enables estimation of the non-integer part of the shift, which improves the precision of the sub-pixel shift.

We present an evaluation of the proposed method using standard images with different rotations and scales. The comparison of the estimation errors demonstrates that the proposed method achieves correct shift estimation for the degree of the scale and rotation. In addition, the results indicate that the proposed method is robust compared to feature-based and intensity-based approaches.

2. PREVIOUS ALGORITHM

2.1. Rotation and scale in log-polar transform

We define image $X_F(x, y)$ and its translation $X_G(x, y)$ using scale factor S , shift (δ_x, δ_y) , and rotation angle θ_0 as follows:

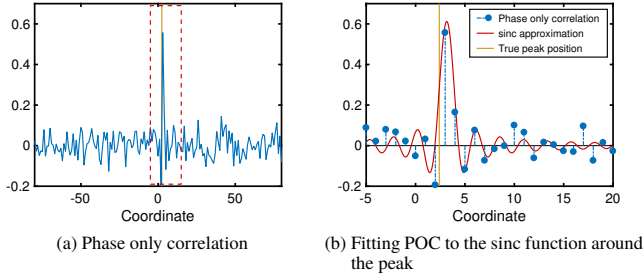


Fig. 1. Peak expression in the POC and its approximation by sinc function

$$X_G(x, y) = X_F(Sx \cos \theta_0 - Sy \sin \theta_0 - \delta_x, \\ Sx \sin \theta_0 + Sy \cos \theta_0 - \delta_y). \quad (1)$$

Both the images are translated to the frequency domain by Fourier transform.

$$\mathcal{F}_G(\omega_x, \omega_y) = \frac{1}{S^2} \mathcal{F}_F \left(\frac{\omega_x}{S} \cos \theta_0 - \frac{\omega_y}{S} \sin \theta_0, \right. \\ \left. \frac{\omega_x}{S} \sin \theta_0 + \frac{\omega_y}{S} \cos \theta_0 \right) e^{-j(\omega_x \delta_x + \omega_y \delta_y)} \quad (2)$$

Here \mathcal{F}_F and \mathcal{F}_G denote the 2D Fourier transform of X_F and X_G respectively. Log-polar transform is defined as the coordinate translation of expressions \mathcal{F}_F and \mathcal{F}_G to log distance ρ and angle θ . In other words, ρ and θ are defined by ω_x and ω_y as follows:

$$\rho = \log \left(\sqrt{\omega_x^2 + \omega_y^2} \right), \quad \theta = \tan^{-1}(\omega_x / \omega_y). \quad (3)$$

We express $F(\rho, \theta)$ as the log-polar transform of \mathcal{F}_F and $G(\rho, \theta)$ as the log-polar transform of \mathcal{F}_G . Using these expressions, the relationship of the scaling and rotation (2) is rewritten by the shift in the ρ and θ directions respectively.

$$|G(\rho, \theta)| = \frac{1}{S^2} |F(\rho - \log S, \theta + \theta_0)| \quad (4)$$

2.2. Shift estimation using phase-only correlation

On the basis of the relationship given by (4), the image scale and rotation are obtained by estimating the 1D shift. To estimate the rotation θ_0 , ρ is fixed to 0. Here, we use $F(\theta)$ and $G(\theta)$ to express $F(\rho, \theta)$ and $G(\rho, \theta)$, respectively, with fixed ρ . Note that rotation θ_0 satisfies the following relationship:

$$G(\theta) = F(\theta + \theta_0). \quad (5)$$

The major shift estimation algorithm uses POC. The POC of $F(\theta)$ and $G(\theta)$ is calculated as follows:

$$R(\theta) = \mathcal{F}^{-1} \left(\frac{\mathcal{F}(F(\theta)) \circ \mathcal{F}(G(\theta))^*}{|\mathcal{F}(F(\theta)) \circ \mathcal{F}(G(\theta))^*|} \right). \quad (6)$$

Here, $\mathcal{F}(\cdot)$ denotes the 2D Fourier transform of the matrix, $\mathcal{F}^{-1}(\cdot)$ is the inverse 2D Fourier transform, \circ is element-wise matrix multiplication (division is also calculated in an element-wise manner), and $\mathcal{F}(G)^*$ is the complex conjugate of $\mathcal{F}(G)$.

POC $R(\theta)$ has a peak according to the shift of the images. Figure 1(a) shows the POC characteristics, where the blue line represents the POC with a peak according to the shift (the yellow line). To search the best location of the peak, POC $R(\theta)$ is fitted to a shift of the sinc function. The approximation result of the sinc function is shown as the red line in Fig. 1(b). In addition to the rotation, scale S can be estimated by fixing θ and fitting the 1D POC between $F(\rho)$ and $G(\rho)$.

In practice, log-polar transform is conducted on the discrete image; therefore, the value of angle θ is quantized into the multiply of the step θ_{step} . In the discrete expression, the precision of the non-integer shift is limited if the estimation is given by fitting the POC to the model function because the true peak of the POC may not appear in the discrete expression and the peak of the model function does not match the peak of the POC.

3. PROPOSED METHOD

Log-polar transform is the translation of image frequency $\mathcal{F}_F(\omega_x, \omega_y)$. This transform requires interpolation of the image frequency to obtain the specified frequency component $F(\rho, \theta)$; however, interpolation of the frequency component causes a large error, particularly in the high-frequency component. To suppress this interpolation error, we propose a new rotation estimation algorithm using Radon transform.

3.1. Radon-transform-based rotation and scale estimation

The Radon transform $F(\rho, \theta)$ of image $X_F(x, y)$ is calculated by summing all pixels along angle θ .

$$F(\rho, \theta) = \int_{-\infty}^{\infty} X_F(\xi \cos \theta - \rho \sin \theta, \xi \sin \theta + \rho \cos \theta) d\xi \quad (7)$$

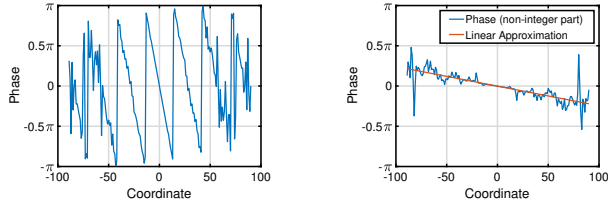
Similarly, Radon transform $G(\rho, \theta)$ is calculated from $X_G(x, y)$. In Radon transform F , G , shift (δ_x, δ_y) , scaling S , and the rotation θ_0 become

$$G(\rho, \theta) = \frac{1}{S} F \left(S\rho - \sqrt{\delta_x^2 + \delta_y^2} \sin \left(\theta - \tan^{-1} \frac{\delta_y}{\delta_x} \right), \theta + \theta_0 \right). \quad (8)$$

This equation means that the rotation of two images is expressed as the 1D shift for the θ direction. Here, the rotation is expressed as 1D scaling for the ρ direction. Using this feature, we estimate rotation θ_0 using the 1D shift estimation algorithm. Note that the estimation based on Radon transform does not depend on scale factor S and shift (δ_x, δ_y) ; therefore, we adjust shift (δ_x, δ_y) by shifting the centroids of the images and calculate the Radon transform at $\rho = 0$. We obtain $F(0, \theta)$ and $G(0, \theta)$. If we express $F(0, \theta)$ and $G(0, \theta)$ as $F(\theta)$ and $G(\theta)$ respectively, the rotation estimation can be expressed as follows:

$$G(\theta) = F(\theta + \theta_0) \quad (9)$$

The proposed Radon transform uses spatial image $X_F(x, y)$ rather than its frequency $\mathcal{F}(\omega_x, \omega_y)$. This eliminates the need to interpolate the frequency components. In addition, Radon transform adds all pixels along the specified angle θ . This operation reduces the influence of interpolation error that occurs in the points that are distant from a pole.



(a) Wrapped phase components with integer shift (b) Unwrapped phase component and its linear approximation

Fig. 2. Linear approximation for the phase of non-integer shift

3.2. Sub-pixel shift estimation by linear approximation of the phase component

As discussed in Section 2.2, the precision of the non-integer part of shift θ_0 given by POC is uncertain. To improve the estimation of the non-integer shift, we introduce a non-integer shift estimation based on linear approximation of the phase component. We express the phase component of the correlation of $F(\theta)$ and $G(\theta)$ as $C(k)$.

$$r(k) = \frac{\mathcal{F}(F(\theta)) \circ \mathcal{F}(G(\theta))^*}{|\mathcal{F}(F(\theta)) \circ \mathcal{F}(G(\theta))^*|}, C(k) = \tan^{-1} \frac{\Im(r(k))}{\Re(r(k))} \quad (10)$$

$\Re(\cdot)$, $\Im(\cdot)$ denote the real and imaginary parts of the content, respectively. The correlation $C(k)$ can be approximated by the following linear expression:

$$C(k) \simeq a \cdot k \quad (11)$$

Thus, the coefficient a can be estimated by the following linear regression.

$$a = \operatorname{argmin}_a \sum_k (C(k) - a \cdot k)^2 \quad (12)$$

However, the output range of \tan^{-1} in (10) is limited to the range $[-\pi, \pi]$. As a result, $C(k)$ becomes the wrapped form shown in Fig. 2 (a). To address this issue, we split phase component C into an integer component C' and a decimal component C'' .

$$C'(k) \simeq a'k, \quad C''(k) \simeq a''k \quad (13)$$

$$C(k) = C'(k) + C''(k) \quad (14)$$

A diagram of the shift estimation splitting the integer and non-integer components is shown in Fig. 3. First, we estimate integer component a' by searching the peak of the conventional POC. Then, we subtract the phase of the integer shift from $C(k)$. We then obtain the phase of the decimal component $C''(k)$.

$$C''(k) = C(k) - a'k \quad (15)$$

Note that this expression does not contain the wrapping effect as shown in Fig. 2 (b). By modifying the minimization (12) to the estimation of the non-integer part, we obtain the minimization of a'' as follows:

$$a'' = \operatorname{argmin}_a \sum_k (C''(k) - a \cdot k)^2 \quad (16)$$

By combining integer shift a' and non-integer shift a'' from (16), we obtain image rotation θ_0 as follows:

$$\theta_0 = a\theta_{\text{step}} = (a' + a'')\theta_{\text{step}} \quad (17)$$

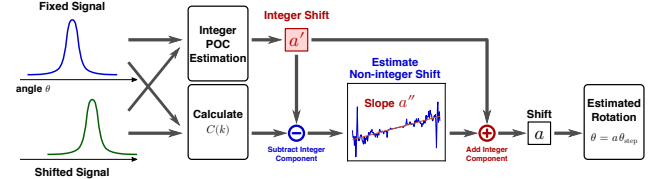


Fig. 3. Sub-pixel shift estimation for the Radon transformed axis

3.3. Radon-transform-based scale estimation

Using the rotation estimation described in the previous section, we obtain the Radon transform of the image with adjusted rotation.

$$G'(\rho, \theta) = G(\rho, \theta - \theta_0) = \frac{1}{S} F(S\rho, \theta)$$

We can obtain scale factor S by calculating the ratio of coordinates whose values exceed a specified threshold. In other words, we express ρ_{F1} as the first coordinate whose value $F(\rho_{F1}, \theta)$ exceeds the threshold and ρ_{F2} as the last coordinate where $F(\rho_{F2}, \theta)$ exceeds the threshold. Similarly, we express ρ_{G1} , ρ_{G2} for the coordinate of $G(\rho, \theta)$. The estimate of the scale is obtained as follows:

$$S \simeq \frac{\rho_{G1} - \rho_{G2}}{\rho_{F1} - \rho_{F2}} \quad (18)$$

To reduce interpolation error and calculation cost, we use the ρ -axis of the Radon transform in $\theta = 0^\circ$ and $\theta = 90^\circ$. Note that we selected transform angles $\theta = 0^\circ$ and $\theta = 90^\circ$ because Radon transform can be calculated with less interpolation error with these angles.

4. EVALUATION

4.1. Experimental settings

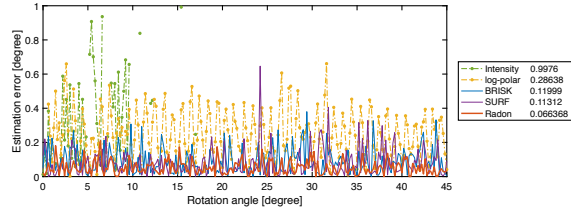
To evaluate the proposed algorithm, we compared rotation and scale estimation for standard images. The images were rotated and scaled with a specified angle and scale value. Then, the estimation algorithm was applied, and the error between the estimated and ground-truth values was calculated. In this evaluation, we used 14 images with size 256×256 and 11 images with size 512×512 . To compare the precision of the rotation estimation algorithm, images were rotated from 0° to 45° at steps of 0.2° . In addition, scales of 0.6, 0.8, and 1.0 were tested. When we compare scale estimation precision, the input rotation was fixed at 35° and the input scale was varied from 0.6 to 1.0 at a step of 0.01. To evaluate estimation robustness, white Gaussian noise was added to the fixed and shifted images. The standard deviation of the Gaussian noise was $\sigma = 0$ (no noise), $\sigma = 10$, and $\sigma = 20$. We compared the proposed algorithm to the conventional estimation algorithm, two feature-based algorithms, i.e., SURF [11] and BRISK features [12], the intensity-based algorithm using Mattes' mutual information [6], and the POC-based algorithm using log-polar transform [3].

4.2. Rotation estimation error

Table 1 shows the rotation estimation errors for each scale. Note that the errors of all images are averaged. The proposed Radon-based method yielded higher precision, particularly with small-scale images. The results demonstrate that the proposed method can estimate

Table 1: Comparison of average errors of rotation estimation for all images

Size	Scale	SURF	BRISK	Intensity	Log-polar	Proposed
256	0.6	0.6768	0.6539	1.0726	0.4792	0.0901
	0.8	0.2257	0.1735	0.6262	0.3355	0.0725
	1.0	0.0945	0.0669	0.3128	0.1615	0.0687
512	0.6	0.1205	0.1116	1.0361	0.4830	0.0849
	0.8	0.0594	0.0866	0.7625	0.3168	0.0818
	1.0	0.0286	0.0258	0.4031	0.2707	0.0786
Average		0.2252	0.1879	0.6964	0.3382	0.0790

**Fig. 4.** Rotation errors for the rotation estimation of Milkdrop image (scale 0.6)**Table 2:** Comparison of average errors of rotation estimation for noisy images with a standard deviation of 10

Size	Scale	SURF	BRISK	Intensity	Log-polar	Proposed
256	0.6	0.7669	1.3115	1.0359	0.4837	0.1378
	0.8	0.2624	0.3361	0.6157	0.3487	0.1236
	1.0	0.1224	0.1224	0.3244	0.2150	0.1192
512	0.6	0.1250	0.1339	1.0271	0.4140	0.1106
	0.8	0.0701	0.0744	0.7559	0.3063	0.1067
	1.0	0.0371	0.0402	0.4248	0.2726	0.1060
Average		0.2590	0.1847	0.6901	0.3417	0.1191

rotation regardless of scale. In addition, the proposed method outperformed the log-polar and feature-based methods, i.e., SURF and BRISK.

The rotation estimation errors for the Milkdrop image (scale 0.6) are shown in Fig. 4. As can be seen, BRISK features achieve the higher estimation precision than SURF features. However, the number of BRISKS tend to be small, and estimation fails if the number of keypoints is less than three. The intensity-based method estimates with the lower error under 15° ; however, estimating larger angles is difficult, and an inappropriate local solution produces a large estimation error.

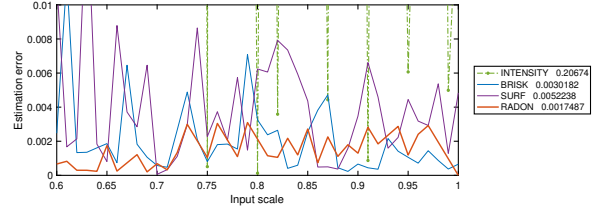
Table 2 compares the rotation estimation errors for the noisy images (standard deviation $\sigma = 10$). As can be seen, the proposed method achieves rotation estimation that is robust against noise, and feature-based methods return large estimation errors because of the small number of feature points.

4.3. Scale estimation error

The scale estimation errors rotated by 35° are compared in Table 3. These results demonstrate that the proposed Radon-based transform can estimate the image scale with less error compared to feature-based and intensity-based methods, particularly when the image size is 256. The proposed method takes the average of two scale estimations to reduce the estimation error, which improves estimation precision for images of size 512. Figure 5 compares the scale estimation errors for the Milkdrop image. The proposed algorithm demonstrates higher estimation precision when the input scale is in the range of 0.6 to 0.7.

Table 3: Comparison of scale estimation errors for images rotated by 35° .

Size	SURF	BRISK	Intensity	Proposed
256	0.00361	0.00237	0.27234	0.00174
512	0.00098	0.00088	0.27073	0.00092
Average	0.00240	0.00169	0.27160	0.00136

**Fig. 5.** Comparison of errors of scale estimation for Milkdrop image with rotation angle 35° **Table 4:** Comparison of execution times for rotation and scale estimation

Size	Scale	SURF	BRISK	Intensity	Log-Polar	Proposed
256	0.6	0.0452	0.3161	0.8353	0.0214	0.0149
256	0.8	0.0427	0.4650	0.9745	0.0261	0.0150
256	1.0	0.0482	0.5050	1.0480	0.0363	0.0182
512	0.6	0.0874	0.4451	2.4960	0.0709	0.0311
512	0.8	0.0989	0.4477	2.8349	0.0871	0.0367
512	1.0	0.1230	0.4864	3.1434	0.1170	0.0471

In this range, it is difficult for the feature or intensity-based methods to estimate the scale value accurately.

4.4. Execution time

We compared the comparison of the execution times of the rotation and scale estimation algorithms. All angles were evaluated from 0° to 45° in 0.2° steps, and the results were averaged. The rotation and scale estimation for each image size (256 and 512) and for each scale (0.6 to 1.0) are compared in Table 4. For all image sizes and scales, compared to the conventional methods, the proposed method demonstrates a faster execution time because the Radon transform calculation is limited to three axes, and each estimation is processed in 1D signals.

5. CONCLUSION

In this paper, we have proposed a rotation and scale estimation algorithm based on Radon transform and sub-pixel shift estimation. Radon transform can reduce the influence of interpolation error because it is applied to a spatial image rather than the frequency. The number of ranges of Radon transform can be limited to $\rho = 0$, $\theta = 0^\circ$, and $\theta = 90^\circ$, therefore, the proposed method has an advantage relative to computational cost. As well as introducing the Radon transform, we have proposed a sub-pixel shift estimation method that uses linear approximation of the phase component, which enables an accurate non-integer shift. In the proposed method, we have combined the conventional POC method for the integer part of the shift and linear approximation for the non-integer part. Evaluations using test image demonstrate that the proposed method accurately estimates rotation regardless of the degree of the input rotation, scaling, and shifting. In particular, compared to other conventional approaches, the proposed method realizes robust estimation when the input scale differs from 1 or noise is added to the images.

6. REFERENCES

- [1] M. Balci and H. Foroosh, "Subpixel estimation of shifts directly in the fourier domain," *IEEE Transactions on Image Processing*, vol. 15, no. 7, pp. 1965–1972, July 2006.
- [2] T. Dobashi and H. Kiya, "A parallel implementation method of FFT-based full-search block matching algorithms," in *2013 IEEE International Conference on Acoustics, Speech and Signal Processing*, May 2013, pp. 2644–2648.
- [3] Xiaoyong Zhang, Noriyasu Homma, and Kei Ichiji, "A faster 1-D phase-only correlation-based method for estimations of translations, rotation and scaling in images," *IEICE Transactions on Fundamentals of Electronics, Communications and Computer Sciences*, vol. 97, no. 3, pp. 809–819, mar 2014.
- [4] Tatsuhiko Tsuboi and Shinichi Hirai, "Detection algorithm of position and orientation of planer motion objects using Radon transform and one-dimensional phase-only matched filter," *JSME annual Conference on Robotics and Mechatronics (Robomec)*, vol. 2003, no. 2P1-1F-C5, pp. 92, 2003.
- [5] Shinichi Hirai, Tatsuhiko Tsuboi, Akihiko Masubuchi, and Masakazu Zakouji, "Parallel processing of one-sided Radon transform for the detection of the position and the orientation of planar motion objects," *IEICE technical report. Digital signal processing*, vol. 101, no. 384, pp. 31–38, oct 2001.
- [6] David Mattes, David R. Haynor, Hubert Vesselle, Thomas K. Lewellyn, and William Eubank, "Nonrigid multimodality image registration," *Proc.SPIE*, vol. 4322, pp. 4322 – 4322 – 12, 2001.
- [7] M. Styner, C. Brechbuhler, G. Szckely, and G. Gerig, "Parametric estimate of intensity inhomogeneities applied to mri," *IEEE Transactions on Medical Imaging*, vol. 19, no. 3, pp. 153–165, March 2000.
- [8] David G. Lowe, "Distinctive image features from scale-invariant keypoints," *Int. J. Comput. Vision*, vol. 60, no. 2, pp. 91–110, Nov. 2004.
- [9] P. Thevenaz and M. Unser, "A pyramid approach to sub-pixel image fusion based on mutual information," in *Proceedings of 3rd IEEE International Conference on Image Processing*, Sept 1996, vol. 1, pp. 265–268 vol.1.
- [10] P. Thevenaz, U. E. Ruttimann, and M. Unser, "A pyramid approach to subpixel registration based on intensity," *IEEE Transactions on Image Processing*, vol. 7, no. 1, pp. 27–41, Jan 1998.
- [11] Herbert Bay, Andreas Ess, Tinne Tuytelaars, and Luc Van Gool, "Speeded-up robust features (surf)," *Computer Vision and Image Understanding*, vol. 110, no. 3, pp. 346 – 359, 2008, Similarity Matching in Computer Vision and Multimedia.
- [12] S. Leutenegger, M. Chli, and R. Y. Siegwart, "Brisk: Binary robust invariant scalable keypoints," in *2011 International Conference on Computer Vision*, Nov 2011, pp. 2548–2555.
- [13] M. Muja and D. G. Lowe, "Fast matching of binary features," in *2012 Ninth Conference on Computer and Robot Vision*, May 2012, pp. 404–410.
- [14] Marius Muja and David G. Lowe, "Fast approximate nearest neighbors with automatic algorithm configuration," in *In VIS-APP International Conference on Computer Vision Theory and Applications*, 2009, pp. 331–340.
- [15] Hiroshi Sasaki, Koji Kobayashi, Takafumi Aoki, Masayuki Kawamata, and Tatsuo Higuchi, "Rotation measurements using rotation invariant phase only correlation," *ITE Technical Report*, vol. 22, no. 45, pp. 55–60, sep 1998.
- [16] Sei Nagashima, Koichi Ito, Takafumi Aoki, Hideaki Ishii, and Koji Kobayashi, "A high-accuracy rotation estimation algorithm based on 1D phase-only correlation," in *Image Analysis and Recognition: 4th International Conference, ICIAR 2007, Montreal, Canada, August 22-24, 2007. Proceedings*, Mohamed Kamel and Aurelio Campilho, Eds., Berlin, Heidelberg, 2007, pp. 210–221, Springer Berlin Heidelberg.